Available online at www.sciencedirect.com

SciVerse ScienceDirect

Ceramics International 38 (2012) 3869–3873

CERAMICS INTERNATIONAL

www.elsevier.com/locate/ceramint

Effects of sulfidation on the optoelectronic properties of hydrothermally synthesized ZnO nanowires

Ian Y.Y. Bu [a,*], Yih-Min Yeh [b]

[a] Department of Microelectronics Engineering, National Kaohsiung Marine University, 81157 Nanzih District, Kaohsiung City, Taiwan, ROC

[b] Graduate School of Opto-Mechatronics and Materials, Wufeng University, 117, Sec 2, Chiankuo Rd., Minhsiung, Chiayi County 62153, Taiwan, ROC

Received 21 December 2011; received in revised form 13 January 2012; accepted 13 January 2012

Available online 23 January 2012

Abstract

Zinc sulfide is an important material for wide range of applications. In this study, we have developed an environmentally friendly and direct method for converting the outer shells of zinc oxide nanowires into zinc sulfide. Such method can effectively replace traditionally used H_2S which is toxic. It was found that the conversion of ZnO into ZnS take place below melting point of sulfur at around 400 °C. It was also found oxygen play an important role in sulfidation as it can only occur through O out diffusion.

Keywords: A. sol–gel process; A. Sintering; D. ZnO; B. Nanocomposites

1. Introduction

Zinc oxide (ZnO) is a wide bandgap 3.37 eV semiconductor with large exciton binding energy of 60 meV at room temperature, has been extensively investigated due to its versatile applications in photocatalysis, humidity sensor, piezoelectric materials and solar cells [1–6]. Recently, stimulated by their potential enhancement in various optoelectronic devices, ZnO nanostructures have also attracted great attention of researchers [7–11].

Although high quality ZnO nanostructures have been successfully synthesized by using the CVD process [12,13], excessive process temperature and expensive vacuum technologies can limit the substrate selection and large scale scaling in production process. The current study considers the Hydrothermal growth of ZnO nanostructures, which offers several process advantages such as relatively low deposition temperature (<90 °C) and inexpensive set-up. A typical hydrothermal growth of ZnO nanostructures involves two fundamental steps [14]; namely seed preparation and nanostructure growth. Usually, ZnO seed are prepared by dissolving ZnO in ethanol solutions and then heated up in order to form colloidal seeds. Subsequently, the seed-coated substrate is transferred into a nutrient solution that consists of excessive ammonia and zinc nitrate. The key processing parameters include, seed preparation, heating methods, pH, and chemical compound concentrations. It should be noted that the diameter of ZnO nanostructures can be controlled by the initial seed solution [14]. To a certain extent, ZnO nanowire lengths can be controlled by deposition time although growth rate usually saturated over time [14].

In general, the optoelectronic properties of ZnO are strongly influenced its size, morphology and crystal orientation [15]. One of the important processing advantages ZnO process possess over other materials is the possibility of synthesizing several different types of nanostructure. These allotropes includes nanowires [16,17], nanotubes [18,19], nanoflowers [19], nanoplates [19,20] and tetrapods [21,22]. Furthermore, the electrical, optical and magnetical properties of ZnO nanostructures can be modified via impurity doping and surface modification. Successful demonstrations includes Cu and Mn addition into ZnS nanowires [23], Co incorporation to produce diluted magnetic ZnO:Co nanowires [24,25] and the Al doping to enhance n-type characteristics of the nanowires [26,27]. The focus of the paper is upon the sulfidation of ZnO nanowires. In the literature, two strategies have been employed for surface modification of ZnO nanowires; namely, the direct conversion and the capping via further processing steps [28,29].

* Corresponding author. Tel.: +886 97250 6900; fax: +886 73645589.
E-mail address: ianbu@hotmail.com (I.Y.Y. Bu).

0272-8842/$36.00
doi:10.1016/j.ceramint.2012.01.038

In order to produce ZnS (zinc sulfide), the direct synthesis involves thermally annealing the sample under H_2S atmosphere [30,31], whereas capping can be achieved through chemical treatment by using S-containing compounds such as NaS. Although these methods are effective to produce ZnS coated ZnO, both methods utilize severe hazardous chemical compounds and therefore unsuitable for industrial scaling. For example, NaS is a volatile chemical that can auto-ignite and releases poisonous H_2S gas. Consequently, it would be desirable to replace the sulfurization process with a less hazardous alternative, such as sulfur. Indeed, from the safety point of view, elemental sulfur is more stable and environmentally friendly. Effects of elemental sulfurization treatment on surface morphology, structural properties, electrical transport and room temperature PL of ZnO nanowires are also investigated by the study.

2. Experimental

All chemicals were purchased from Sigma–Adrich and used as received without further purification. ZnO nanowires were hydrothermally synthesized through the two step process; seed layer deposition and nanowire growth. Firstly, the seed layer was prepared by dissolving 0.1 M of zinc acetate in IPA by using a magnetic stirrer without external heating. Subsequently, the prepared seed solution was dispersed onto soda lime glasses using a spin coater at 5000 rpm for 30 s. After the deposition, the thin film layer was preheated at 300 °C on a hotplate. The spin coat/heating cycle had been repeated for three times in order to ensure a good adhesion of the seed layer. Following the seed layer formation, the glass substrates were vertically suspended and transferred into the nutrient bath. The nutrient bath, which consists of equal molar of zinc nitrate and hexamine. Then ZnO nanowires were then hydrothermally grown for 2 h on a hotplate set at 90 °C. The hydrothermal growth were terminated by removing the sample from the bath, thoroughly washed with D.I. water and blown dry using a pressurized high purity nitrogen flow.

For hydrothermally grown ZnO nanowires, the sulfurization was carried out within a two-zones vacuum furnace in order to convert them into zinc sulfide coated NW. At one zone sulfur powder was placed, and in the other zone ZnO NW was located. The sulfur powder zone was heated up to 240 °C, the sample zone was heated up to 300 and 400 °C and then allowed to cool down naturally to room temperature after the sulfurization. The process temperature was deliberately kept below elemental sulfur melting point 444.6 °C.

The chemical composition, size and surface morphology of the ZnO nanowire samples have been evaluated by using an FEI Quanta 400 F Environmental Scanning Electron Microscope (ESEM), equipped with an Energy Dispersive Spectroscopy EDS. The structure and crystal orientation were measured by the Siemens D5000 X-Ray Diffractometer which uses the Cu Kα radiation. Raman spectroscopy and photoluminescence of the thin films were conducted by the Dongwoo Macro Raman spectrometer/PL system at room temperature. Electrical *I–V* measurements were taken by source meter (Keithley 2400). In order to ensure a good Ohmic contacts to the fabricated device the front electrodes were formed by DC sputtering of the ITO target through metal masks defined with 60 μm diameter. Prior to the measurement the back contacts were made by applying commercially available silver paste on the highly conductive P-type Si substrate.

3. Results and discussion

Fig. 1(a–c) shows the SEM images of the untreated ZnO nanowire and samples sulfurized at different temperatures (300 and 400 °C). The approximate length and diameter of the nanowires are around 500 nm and diameter of 50 nm, respectively. At a closer inspection of the tip of the Zn nanowires, enables us to observe a clear hexagonal shaped tip, which can confirm the wurtztze structure of the ZnO nanowire. Fig. 1a shows the untreated ZnO nanowire sulfurized, which are well separated and without agglomeration. However, ZnO nanowire sulfurized at 300 °C clearly shows bundled ZnNW, with (2–3) ZnNW fused together. This bundleling of ZnO nanowires was accompanied with a formation of large particles on the ZnNW surface. As the sulfurization temperature increases to 400 °C, the ZnNW appears unbundled with a visible decrease in particle formation.

Fig. 2(a–c) shows the XRD spectra of as deposited (insert) and sufurization ZnO nanowire at 300 °C and 400 °C, respectively. As deposited sample showed a strong XRD peak at around 34.44°, which indicate that there is preferential orientation with the *c*-axis perpendicular (0 0 2) orientation to the substrate. It can be observed from the relative XRD intensities after thermal annealing in S environment at 300 °C, the XRD peaks appeared at 34.42° (0 0 2), 36.29° (1 0 1), 56.68° (1 1 0) and 61.70° (1 0 3). It is observed that the intensity of ZnO peaks have decreased, along with the appearances of ZnS peaks at 47.50° (1 1 0). As the sulfurization reaches 400 °C, one can observe appearance of additional ZnS XRD peak at around 28.67° (0 0 2). The mechanisms behind the appearance of ZnS XRD peaks will be further discussed at latter part of this paper.

EDS compositional analysis were performed in order to gain insights into the mechanism behind the sulfurization of Znnw. Table 1 shows the EDS analysis of the untreated ZnNWs and sulfurized at 300 and 400 °C. The as deposited ZnNW is oxygen rich with a Zn/O ratio of 44:56. In general, hydrothermal grown ZnO NW tends to be oxygen rich due to the incomplete reaction on the ZnO surface. As the sulfurization temperature increases from 300 °C to 400 °C, there is a slight increase in sulfur incorporation from 2.73% to 3.34%. Fig. 3 shows the typical EDS mapping of ZnNW Sulfurized at 400 °C. As expected, Zn, O and S elements were detected. It is reassuring that most of the S are situated on ZnO nanowire which indicate S incoporation.

Accordingly, the increase in sulfur is accompanied with the decrease in oxygen content. Based on the structural and composition analysis, a growth model is proposed for the incorporation of elemental S into ZnNW. Generally, a successful conversion from Zinc oxide surface to zinc sulfide

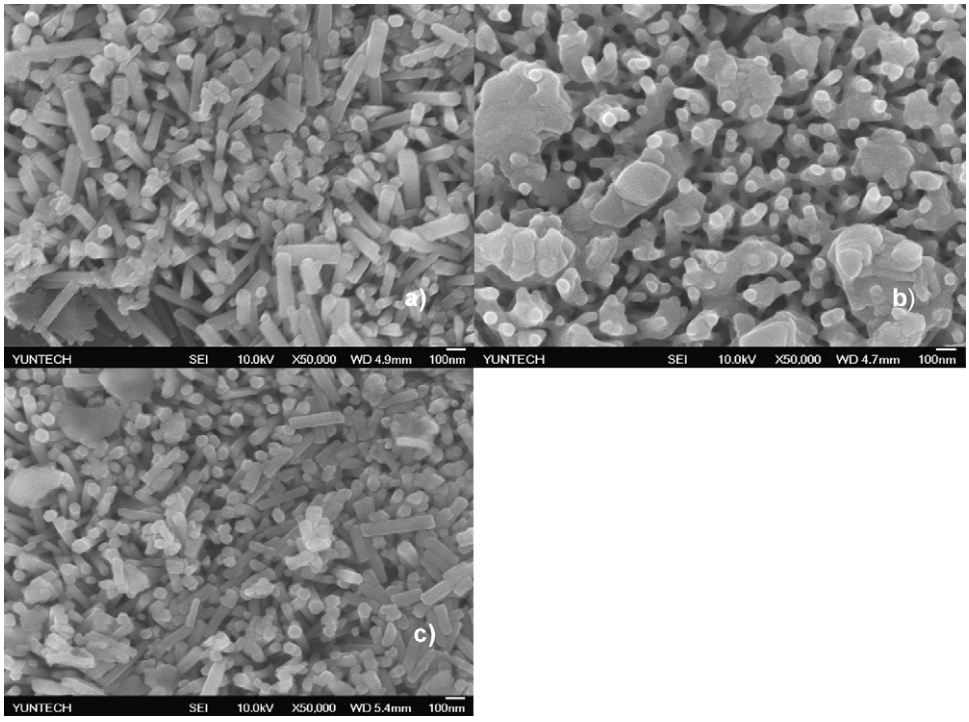

Fig. 1. SEM image of (a) as deposited ZnO nanowire (b) ZnO nanowire sulfurized at 300 °C and (c) ZnO nanowire sulfurized at 400 °C.

involves a substitution between oxygen with sulfur. This substitution process occurs over several stages: (1) diffusion of sulfur into the ZnO surface (2) exchange of oxygen with sulfur; and (3) out diffusion of oxygen. Clearly, the diffusion of S into ZnO is temperature dependent. In order to decide the rate limiting of the sulfurization step it is necessary to consider the compositional detail. Clearly, the EDX data suggests that the ZnO–ZnS conversion occurs through oxygen out diffusion and sulfur incorporation. Another observed tendency is the much faster out diffusion of O compared to S, which indicates a much higher oxygen diffusion coefficient. As expected, due to the radii of oxygen atoms being much smaller than those of atomic S, the out-diffusion of oxygen is much faster than S. It is interesting to note, such trend has not been reported in the ZnO

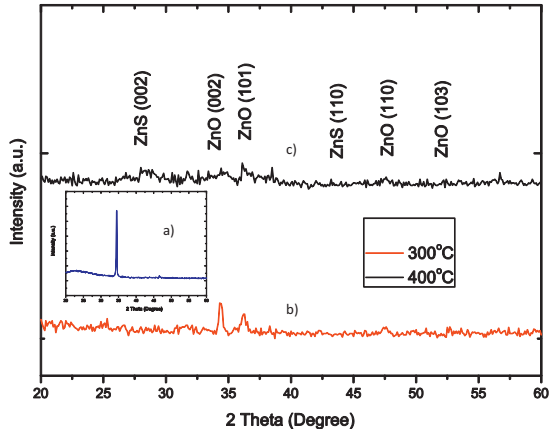

Fig. 2. XRD peaks of the as deposited (a) ZnO nanowire(insert), (b) sulfurized at 300 °C and (c) 400 °C.

sulfidation experiements by using H_2S. The difference can be attributed to a much higher reactivity of H_2S than elemental S. In the case of using H_2S, the hydrogen assists the creation of oxygen vacancies through reduction and as a result, encourages an efficient substitution with S. Similarly, $NaS{:}9H_2O$ decomposes into toxic HS and sulfidize to facilitate sulfidation. Such a mechanism is unavailable in sulfidation using elemental S. Instead the control of out diffusion of oxygen to S in diffusion becomes more significant. As the suphurization temperature is increased to 300 °C, small ZnS XRD peaks occurs due to the diffusion of S. It is interesting to note that several large aggromerates have appeared on ZnNW sufurized at 300 °C. These aggromerate were caused by insufficient oxygen vacancy to accomadate S diffusion into the ZnO.

As the sulfudization temperature is raised to 400 °C, which enables a much faster out-diffusion of O than S and resulted in increase in S content. Clearly, the conversion process is oxygen vacancy driven. When ZnNW sulfidized at 400 °C, there are significant decrease in S agglomerates on the ZnO nanowire surface accompanied without significant decrease in S content on the SEM image, which suggests that some of the S gained sufficient energy from the furnace and diffuse into ZnO surface.

Table 1
EDS composition of the as deposited ZnO nanowire, Sulfurized 300 °C and sulfurized 400 °C.

Sample	Zn	O	S
As deposited	44	56	0
Sulfurized at 300 °C	38.28	58.99	2.73
Sulfurized at 400 °C	41.23	55.43	3.34

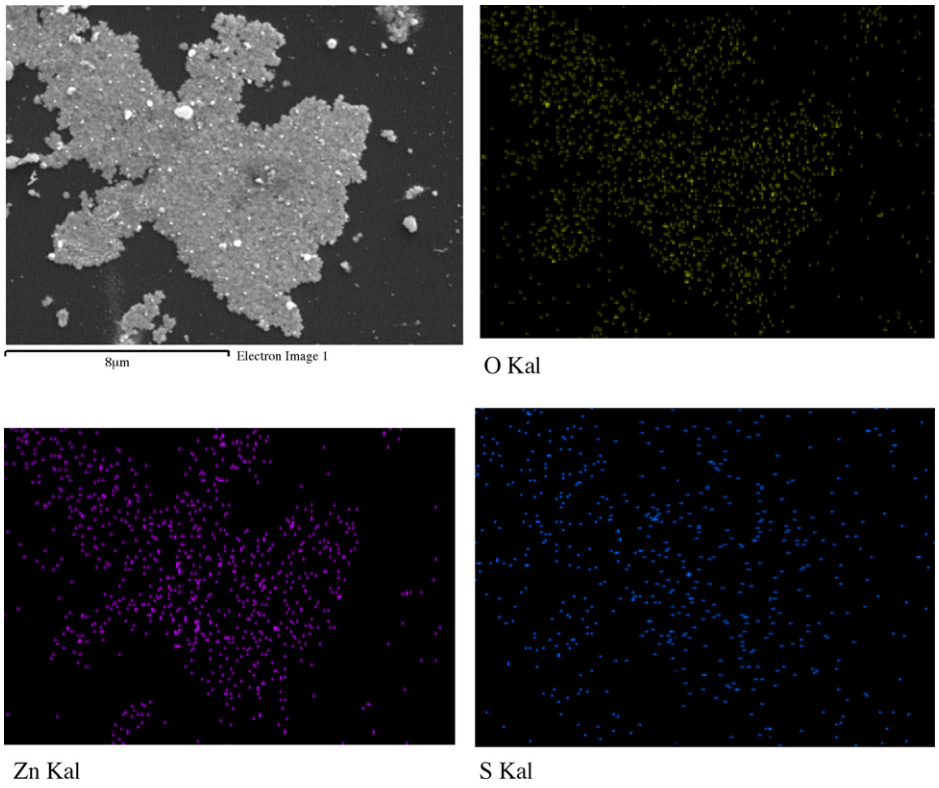

Fig. 3. EDS mapping of the ZnO nanowire sulfurized at 400 °C.

Indeed, the enhancement of ZnS XRD peaks suggests that the formation of ZnS through thermal annealing restructuring. The optical properties of the sufurized ZnNWs were investaigated by PL spectroscopy at room temperature. Fig. 4(a–c) shows the PL property of the untreated and thermally sulfurized ZnNW at 300 °C and 400 °C, respectively. Generally, two peaks centred at around 380 nm and 500 nm are associated with ZnO. The emission peak at 380 nm originates from UV emission from the recombination of free excitons process [32].

There is an additional emission around 550 nm assigned to defective oxygen vacancies. Fig. 4b shows that ZnNW sufurized at 300 °C exhibit a sharp UV emission peak and a broad visible emission peak. The relative large visible emission peak suggests ZnNW sufurized at 300 °C contains some structural defects. It is interesting to note that the UV peak increases with the sufurization temperature (from 300 °C to 400 °C) of the ZnNW. The enhancement of UV band emission is due to crystallization of ZnO nanowires.

Fig. 5(a and b) shows the dark and photo current voltage characteristic of p-type Si/ZnNW/ZnS (400 °C) heterojunction diode, respectively. The device exhibits a good rectifying behaviour with low leakage current, thus confirming the PN

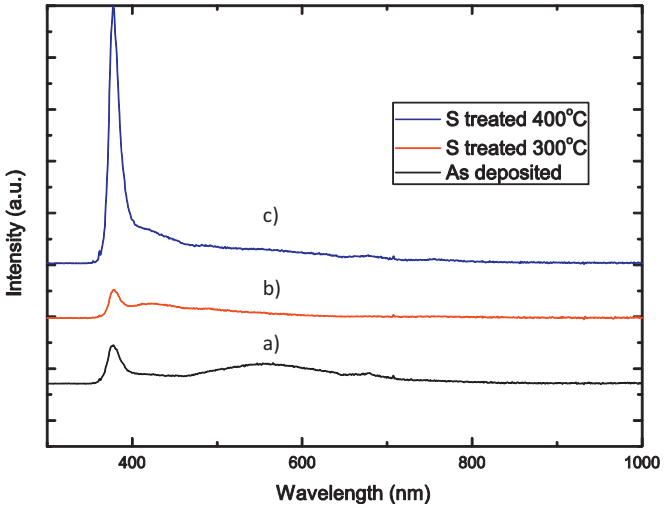

Fig. 4. PL spectra of the (a) as deposited ZnO nanowire (b) ZnO nanowire sulfurized at 300 °C and (c) ZnO nanowire sulfurized at 400 °C.

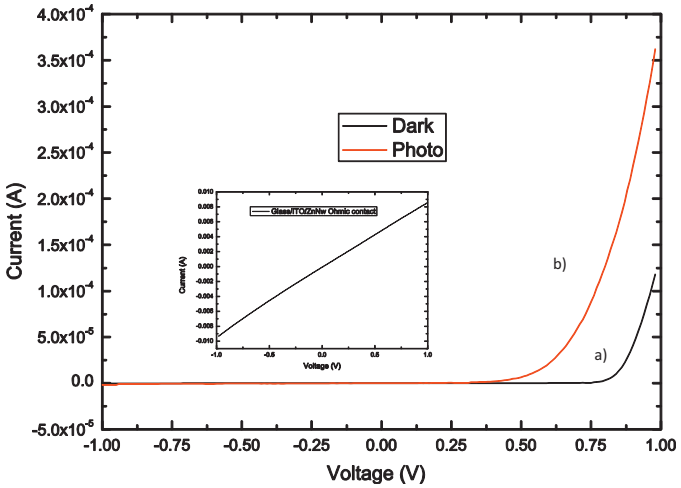

Fig. 5. (a) dark and (b) photo *I–V* characteristics of the p-type silicon/ZnS (sulfurized at 400 °C), respectively. The inset shows the contacts are ohmic.

junction formation. For dark current characteristics, the threshold voltage is around 0.8 V, ON/OFF ratio around 718. Whereas the illuminated device exhibit threshold voltage of 0.68 V and ON/OFF ratio of around 196. The results indicates that ZnNW/ZnS structure is photosensitive and could be of interest in optoelectronic applications such as photoanodes for dye sensitized solar cells and photodetectors.

4. Conclusion

The study examined effects of elemental sulfurization treatment on surface morphology, structural properties, electrical transport and room temperature PL of ZnO nanowires. It can be concluded that the sulfurization process is highly temperature dependant, with an optimal temperature at around 400 °C. The proposed sulfurization mechanism suggests a phenomenon of competitive mechanism between sulfur incorporation and oxygen out diffusion. From industrial processing point of view, the method developed by this study is environmental friendly and should be of interest to next generation ZnO/ZnS devices.

Acknowledgement

The research presented here was undertaken with finance support from the National Science Council, Taiwan, ROC, NSC 99-2628-E-022-001 is gratefully acknowledged.

References

[1] I.Y.Y. Bu, Effect of NH_4OH concentration on p-type doped ZnO film by solution based process, Appl. Surf. Sci. 257 (14) (2011) 6107–6111.
[2] Z.L. Wang, J. Song, Piezoelectric nanogenerators based on zinc oxide nanowire arrays, Science 312 (5771) (2006) 242.
[3] S. Sharma, A. Inamdar, H. Im, B. Kim, P. Patil, Morphology dependent dye-sensitized solar cell properties of nanocrystalline zinc oxide thin films, J. Alloys Compd. (2010).
[4] M.S. Mohajerani, A. Lak, A. Simchi, Effect of morphology on the solar photocatalytic behavior of ZnO nanostructures, J. Alloys Compd. 485 (1) (2009) 616–620.
[5] L. Wang, J. Dai, X. Liu, Z. Zhu, X. Huang, P. Wu, Morphology-controlling synthesis of ZnS through a hydrothermal/solvthermal method, Ceram. Int. (2011).
[6] G.H. Lee, Synthesis and cathodoluminescence of ZnO tetrapods prepared by a simple oxidation of Zn powder in air atmosphere, Ceram. Int. 37 (1) (2011) 189–193.
[7] C. Kuan, M. Hon, J. Chou, I. Leu, Growth characteristics of hierarchical ZnO structures prepared by one-step aqueous chemical growth, Ceram. Int. (2011).
[8] I.Y.Y. Bu, Facile synthesis of highly oriented p-type aluminum co-doped zinc oxide film with aqua ammonia, J. Alloys Compd. (2010).
[9] J.S. Park, T.W. Kim, D. Stryakhilev, J.S. Lee, S.G. An, Y.S. Pyo, D.B. Lee, Y.G. Mo, D.U. Jin, H.K. Chung, Flexible full color organic light-emitting diode display on polyimide plastic substrate driven by amorphous indium gallium zinc oxide thin-film transistors, Appl. Phys. Lett. 95 (1) (2009) 013503.
[10] W. Lim, E. Douglas, D. Norton, S. Pearton, F. Ren, Y.W. Heo, S. Son, J. Yuh, Low-voltage indium gallium zinc oxide thin film transistors on paper substrates, Appl. Phys. Lett. 96 (2010) 053510.
[11] A.K. Zak, M.E. Abrishami, W. Majid, R. Yousefi, S. Hosseini, Effects of annealing temperature on some structural and optical properties of ZnO nanoparticles prepared by a modified sol–gel combustion method, Ceram. Int. 37 (1) (2011) 393–398.
[12] B. Xiang, P. Wang, X. Zhang, S.A. Dayeh, D.P.R. Aplin, C. Soci, D. Yu, D. Wang, Rational synthesis of p-type zinc oxide nanowire arrays using simple chemical vapor deposition, Nano Lett. 7 (2) (2007) 323–328.
[13] S. Wang, X. Jia, P. Jiang, H. Fang, W. Tang, Large-scale preparation of chestnut-like ZnO and Zn–ZnO hollow nanostructures by chemical vapor deposition, J. Alloys Compd. 502 (1) (2010) 118–122.
[14] L.E. Greene, B.D. Yuhas, M. Law, D. Zitoun, P. Yang, Solution-grown zinc oxide nanowires, Inorg. Chem. 45 (19) (2006) 7535–7543.
[15] Z. Fan, J.G. Lu, Zinc oxide nanostructures: synthesis and properties, J. Nanosci. Nanotechnol. 5 (10) (2005) 1561–1573.
[16] H.E. Unalan, P. Hiralal, N. Rupesinghe, S. Dalal, W.I. Milne, G.A.J. Amaratunga, Rapid synthesis of aligned zinc oxide nanowires, Nanotechnology 19 (2008) 255608.
[17] C.H. Lu, Y.C. Lai, R.B. Kale, Influence of alkaline sources on the structural and morphological properties of hydrothermally derived zinc oxide powders, J. Alloys Compd. 477 (1-2) (2009) 523–528.
[18] J. Yang, J. Zheng, H. Zhai, L. Yang, Y. Zhang, J. Lang, M. Gao, Growth mechanism and optical properties of ZnO nanotube by the hydrothermal method on Si substrates, J. Alloys Compd. 475 (1-2) (2009) 741–744.
[19] T.M. Shang, J.H. Sun, Q.F. Zhou, M.Y. Guan, Controlled synthesis of various morphologies of nanostructured zinc oxide: flower, nanoplate, and urchin, Cryst. Res. Technol. 42 (10) (2007) 1002–1006.
[20] S. Shao, P. Jia, S. Liu, W. Bai, Stable field emission from rose-like zinc oxide nanostructures synthesized through a hydrothermal route, Mater. Lett. 62 (8-9) (2008) 1200–1203.
[21] S. Kulkarni, U. Patil, R. Salunkhe, S. Joshi, C. Lokhande, Temperature impact on morphological evolution of ZnO and its consequent effect on physico-chemical properties, J. Alloys Compd. (2010).
[22] J. Jiang, Y. Li, S. Tan, Z. Huang, Synthesis of zinc oxide nanotetrapods by a novel fast microemulsion-based hydrothermal method, Mater. Lett. 64 (20) (2010) 2191–2193.
[23] N. Chien, H. Chung, P. Huy, D.J. Kim, M. Ferrari, Mn, Cu doping and optical properties of highly crystalline ultralong ZnS nanowires, Adv. Mater. Res. 31 (2008) 114–116.
[24] W. Liang, B.D. Yuhas, P. Yang, Magnetotransport in Co-doped ZnO nanowires, Nano Lett. 9 (2) (2009) 892–896.
[25] Y. Tak, K. Yong, A novel heterostructure of Co_3O_4/ZnO nanowire array fabricated by photochemical coating method, J. Phys. Chem. C 112 (1) (2008) 74–79.
[26] D. Lin, H. Wu, W. Pan, Photoswitches, Memories assembled by electrospinning aluminum-doped zinc oxide single nanowires, Adv. Mater. 19 (22) (2007) 3968–3972.
[27] J.B. Shim, H.S. Kim, H. Chang, S.O. Kim, Growth and optical properties of aluminum-doped zinc oxide nanostructures on flexible substrates in flexible electronics, J. Mater. Sci.: Mater. Electron. (2011) 1–7.
[28] S. Senthilkumaar, R.T. Selvi, Synthesis and characterization of one dimensional ZnS nanorods, Synth. React. Inorg. Met.-Org., Nano-Met. Chem. 38 (9) (2008) 710–715.
[29] S. Kar, P. Dutta, T. Pal, S. Ghosh, Simple solvothermal route to synthesize S-doped ZnO nanonails and ZnS/ZnO core/shell nanorods, Chem. Phys. Lett. 473 (1-3) (2009) 102–107.
[30] X.L. Yu, J.G. Song, Y.S. Fu, Y. Xie, X. Song, J. Sun, X.W. Du, ZnS/ZnO heteronanostructure as photoanode to enhance the conversion efficiency of dye-sensitized solar cells, J. Phys. Chem. C 114 (5) (2010) 2380–2384.
[31] M.Y. Lu, J. Song, M.P. Lu, C.Y. Lee, L.J. Chen, Z.L. Wang, ZnO–ZnS heterojunction and ZnS nanowire arrays for electricity generation, ACS Nano 3 (2) (2009) 357–362.
[32] A. Chiappini, C. Armellini, A. Chiasera, M. Ferrari, R. Guider, Y. Jestin, L. Minati, E. Moser, G. Nunzi Conti, S. Pelli, Preparation and characterization of ZnO particles embedded in organic–inorganic planar waveguide by sol–gel route, J. Non-Cryst. Solids 355 (18) (2009) 1132–1135.